THE JOURNAL OF PHYSICAL CHEMISTRY B LETTERS

2006, *110,* 25−29
Published on Web 12/13/2005

Selective Oxidation of Semiconducting Single-Wall Carbon Nanotubes by Hydrogen Peroxide

Yasumitsu Miyata,[†,‡] Yutaka Maniwa,[†,§] and Hiromichi Kataura*[,‡]

Department of Physics, Tokyo Metropolitan University, 1-1 Minami-Osawa, Hachioji, Tokyo 192-0397, Japan, Nanotechnology Research Institute (NRI), National Institute of Advanced Industrial Science and Technology (AIST), 1-1-1 Higashi, Tsukuba 305-8562, Japan, and CREST, Japan Science and Technology Corporation (JST), Japan

Received: October 6, 2005; In Final Form: December 2, 2005

Selective oxidation of single-wall carbon nanotubes (SWCNTs) by H_2O_2 was conducted at varying heating times and monitored by UV−vis−NIR spectroscopy. A major increase in the relative absorption intensity indicated a higher than 80% concentration of metallic SWCNTs in the final product. Here, it is suggested that semiconducting SWCNTs are more reactive than metallic SWCNTs because of hole-doping by H_2O_2, resulting in faster oxidation.

Single-wall carbon nanotubes (SWCNTs) occur as both metal and semiconductor types.[1] However, as yet, none of the synthetic methods used to prepare SWCNTs are in fact selective toward the production of either pure metallic or pure semiconducting SWCNTs. This is a major drawback with regard to applications, where SWCNT purity is essential. For example, metallic SWCNTs are highly desired as nanometer-sized conductors,[2] while semiconducting SWCNTs are required as field effect transistors[3] and saturable absorbers.[4,5] As such, the selective purification of metallic and semiconducting SWCNTs represents a very important target. Thus, many researchers are now focusing their attention on the effective separation and selective isolation of SWCNTs.[6−11]

Hydrogen peroxide is one of the most powerful oxidizers available, and it is widely used in the purification[12] and etching[13] of SWCNTs. Moreover, hydrogen peroxide is also known to decompose thinner SWCNTs much more rapidly by heating and is an effective agent for the diameter-selective purification of SWCNTs.[14,15] The diameter control of semiconducting SWCNTs is particularly important, since the associated band gap is inversely proportional to its diameter. However, little attention has so far been given to the difference in chemical reactivity between metallic and semiconducting SWCNTs in H_2O_2.

Here, we report an optical study of SWCNTs oxidized in H_2O_2. Commercially available HiPco was purified and used as the starting material to obtain SWCNT samples, which were then oxidized in heated H_2O_2. From an analysis of the integrated intensity of the absorption bands of metallic and semiconducting SWCNTs, it was estimated that the concentration of metallic SWCNTs in the final product was higher than 80%. The enrichment of metallic SWCNTs was not observed during oxidation in air. Absorption spectroscopy confirmed that SWCNTs were weakly doped in H_2O_2. It was suggested that the faster oxidation of semiconducting SWCNTs was due to its higher reactivity resulting from hole-doping by H_2O_2.

Raw HiPco SWCNTs were purchased from Carbon Nanotechnologies Inc. (batch #78) and purified by HCl treatment after heating in air.[14] First, the raw HiPco soot was heated at 300 °C for 30 min in air to remove the carbon layers surrounding the Fe nanoparticles (raw soot contains around 30 wt % Fe nanoparticles). The exposed Fe nanoparticles were dissolved by soaking the sample in HCl (18 wt %) at room temperature for 10 min, and the resulting sample was then collected on a membrane and rinsed with purified water. The HCl purification process was repeated two more times, affording a final yield of 60 wt %. The remaining Fe nanoparticle impurities in the SWCNT sample were estimated to be around 4 wt %, as determined from thermogravimetric measurements in air up to 800 °C.

The purified HiPco (4 mg) was dispersed in an aqueous solution of H_2O_2 (30 wt %, 30 mL) for 1 h in an ultrasonic bath at room temperature. The dispersion was then stirred in a preheated water bath at 90 °C. Small aliquots (1 mL) of sample solution were then collected after 15, 25, 32, and 38 min, and the remainder was collected after 47 min. After treatment with H_2O_2, each sample was immediately collected on a membrane and rinsed with purified water. The samples were again soaked in HCl (10 wt %) to remove the remaining Fe nanoparticles. SWCNT thin films were obtained using a procedure based on the filtration method reported by Wu et al.[16] The SWCNTs were dispersed in dimethylformamide (DMF) for 20 min in an ultrasonic bath. The dispersion was filtered down, and the resulting SWCNT film was formed on an omnipore membrane (Millipore, 0.2 μm pore). The SWCNT film on the membrane was transferred directly onto a quartz substrate. After drying the sample for 1 h at 90 °C on a hotplate, the membrane was removed, leaving a thin film of SWCNTs on the substrate. The

* Corresponding author. E-mail address: h-kataura@aist.go.jp. Phone number: +81-29-861-2551. Fax number: +81-29-861-2786.
† Tokyo Metropolitan University.
‡ National Institute of Advanced Industrial Science and Technology (AIST).
§ Japan Science and Technology Corporation (JST).

10.1021/jp055692y CCC: $33.50

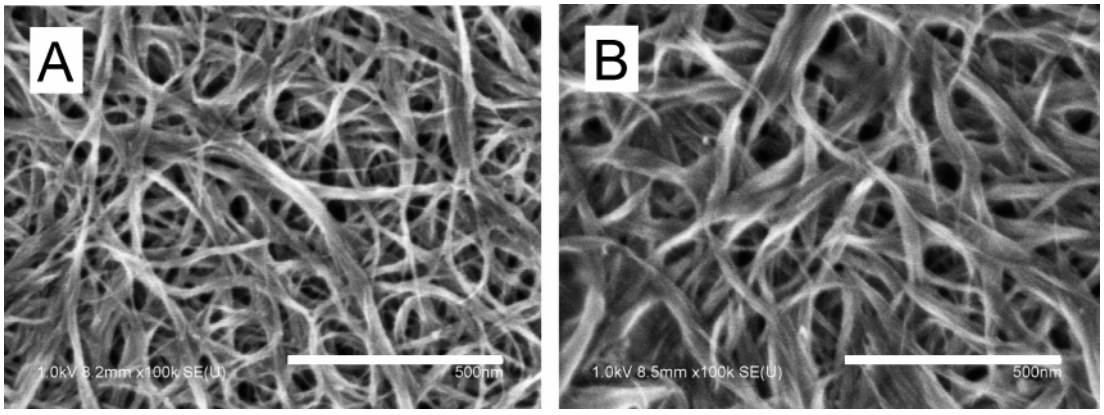

Figure 1. SEM images of the SWCNT films: (A) starting material; (B) after treatment with H_2O_2 for 47 min at 90 °C. The scale bar is 500 nm.

SWCNT films were then heated under vacuum (2×10^{-6} Torr) at 250 °C for 1 h in order to remove the remaining chemicals used in the above treatments. The corresponding images of the resulting thin films were obtained via scanning electron microscopy (SEM, HITACHI S4800). The optical absorption measurements of the SWCNT samples were obtained using a UV−vis−NIR spectrophotometer (SHIMADZU SolidSpec-3700DUV). The Raman spectra were measured at room temperature using a triple monochromator equipped with a CCD detector (Photon Design Co., PDPT3-640S). The samples were exited by an argon ion laser (2.71 eV) and a dye laser (2.06 eV). The same experiments were repeated for another HiPco (lot #R0500 with 20 wt % Fe) to check batch dependence, and the same results were confirmed.

To see the charge-transfer effects induced by H_2O_2 during the above treatments, a well-dried SWCNT thin film was placed in a quartz cell, and its UV−vis−NIR absorption spectra were measured both with and without the presence of a 30 wt % H_2O_2/water solution at room temperature. For comparison with a normal oxidation process, the purified HiPco thin film was heated in air at 420 °C, and the optical absorption spectrum was recorded at room temperature. These measurements were then repeated after heating for 1, 2, and 4 h.

When the purified HiPco dispersion was kept at 90 °C in H_2O_2, the amount of SWCNTs was observed to decrease, resulting in the concomitant formation of gas bubbles in solution. Indeed, the amount of sample remaining after treatment for 47 min is about 1 wt %. The degradation kinetics of SWCNTs in H_2O_2 was strongly dependent on the amount of metal particle catalysts remaining in the sample. For example, raw HiPco containing 30 wt % Fe nanoparticles was completely oxidized, and disappeared in H_2O_2 within 10 min at 90 °C. In contrast, the H_2O_2 treatment of purified SWCNTs produced by laser ablation, in which only a few weight percent of Ni and Co nanoparticles were present, showed minimal reactivity. This clearly shows that the presence of Fe nanoparticles within the samples promoted the oxidation of SWCNTs in H_2O_2. In this oxidation process, it is likely that the decomposition of the hydrogen peroxide was catalyzed by the Fe nanoparticles, and the active oxygen produced was responsible for attacking the SWCNTs. Figure 1 shows an SEM image of the starting SWCNT and H_2O_2-treated (47 min) SWCNT films. The bundle size of the H_2O_2-treated SWCNT was slightly increased. This was caused by an aggregation effect in the solution through the H_2O_2 treatment. The SEM images revealed that both samples contained little amorphous carbon or graphite impurities, indicating that the SWCNTs reacted with H_2O_2 were all converted to gases such as CO or CO_2. Therefore, the H_2O_2-treated SWCNT samples maintained a high degree of purity.

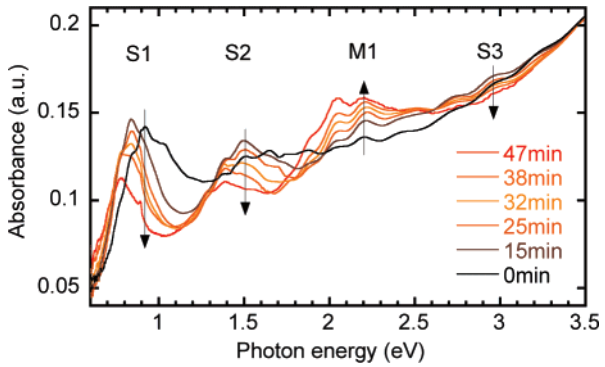

Figure 2. UV−vis−NIR absorption spectra of the H_2O_2-treated SWCNT thin films taken at different treatment times. The arrows indicate the time evolutions of S1, S2, S3, and M1 peaks during the oxidation process.

Figure 2 shows the optical absorption spectra of the SWCNT thin films treated with H_2O_2 at different treatment intervals (spectra were normalized at 3.5 eV). The labels S1 (0.6−1.2 eV), S2 (1.2−1.9 eV), and S3 (2.5−3.3 eV) indicate the exciton optical absorption bands corresponding to the transitions between the van Hove singularities (vHS) of the valence bands and the conduction bands of the semiconducting SWCNTs. The M1 (1.9−2.3 eV) label corresponds to the absorption band of metallic SWCNTs.[17]

In the optical absorption spectra of the H_2O_2-treated SWCNT films, it can be seen that the peak photon energies of the S1 and S2 absorption bands have all shifted to a lower energy as a result of prolonged H_2O_2 treatment. This means that the high-energy side of the S1 and S2 peaks decreased more rapidly than the low-energy side. Here, the higher S1 and S2 absorption energies correspond to the thinner semiconducting SWCNTs in the sample.[17] The observed faster oxidation of thinner SWCNTs is probably caused by their higher C−C bond strain.[18] Consequently, the concentration of larger-diameter semiconducting SWCNTs was increased accordingly. On the contrary, the M1 absorption band indicates only a slight change in peak shape as a result of heat treatment. This implies that diameter-selective oxidation plays only a minor role in the oxidation of metallic SWCNTs, probably due to the very low removal rate. As a result, the intensity of the M1 absorption band increased with increasing oxidation time relative to the S1 and S2 peaks.

Prior to a detailed discussion on the selective oxidation process, it is first necessary to consider the possible effects that change the S1, S2, and M1 absorption conditions. It is well-known that changes in the morphology of SWCNTs have a major effect on their respective absorption spectra. For example, isolated and bundled SWCNTs exhibit different optical absorp-

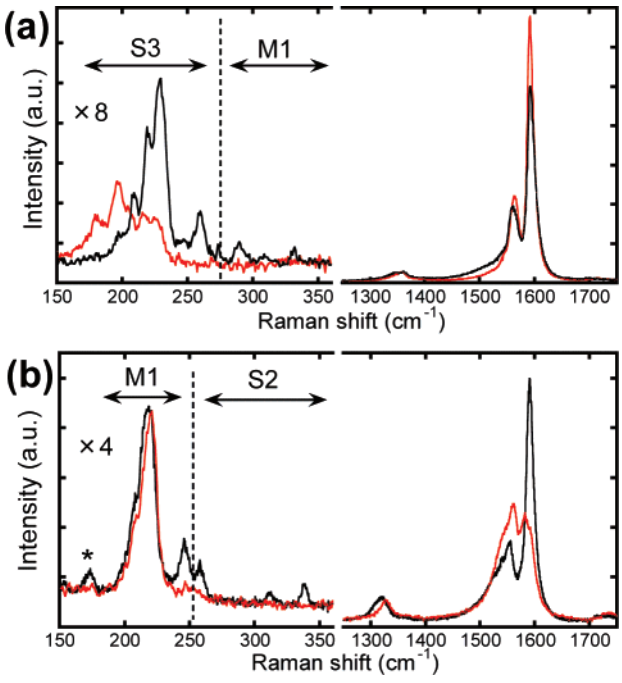

Figure 3. Raman spectra of the SWCNT films: (black) starting SWCNTs; (red) after treatment with H_2O_2 for 47 min at 90 °C. (a) 2.71 eV laser excitation. (b) 2.06 eV laser excitation. The asterisk indicates the peak due to the sideband of the dye laser.

tion spectra.[19] As shown in Figure 1, however, the SWCNT samples used here have the same morphology, since all the SWCNT films were prepared in the same manner. As such, there are no changes expected in the absorption spectra due to morphological changes in the SWCNTs. The charge-transfer effects of HCl, H_2O_2, and DMF are also known to modify the optical absorption properties to some degree.[20] To avoid such effects, the samples were heated to 250 °C under high vacuum prior to taking absorption measurements. Here, it was confirmed that 250 °C is sufficiently high to recover the optical spectra.

Figure 3 shows the Raman spectra of the starting SWCNT and H_2O_2-treated (47 min) SWCNT films. Two excitation energies, 2.71 and 2.06 eV, were used to see a resonance effect. All spectra were normalized by integrated intensity of tangential mode from 1400 to 1700 cm^{-1}, the so-called G-band.[21] Figure 3a indicates the Raman spectra of radial breathing modes[21] (RBMs) and of the G-band for the 2.71 eV excitation. According to the assignment from the wide-range resonance Raman analysis,[22,23] the RBM Raman spectrum is separated into two resonance groups: the resonances of the S3 band (179, 196, 208, 218, and 229 cm^{-1}) and the M1 band (259, 290, 310, and 332 cm^{-1}). In Figure 3b, the RBM spectrum excited by 2.06 eV is separated into the M1 band (220 and 246 cm^{-1}) and the S2 band (258, 311, and 338 cm^{-1}) resonances. Since the RBM spectra in Figure 3a,b have a complementary relationship, the diameter distribution of metallic and semiconducting SWCNTs can be analyzed by connecting these two spectra. For example, the RBM peaks of metallic SWCNTs were observed between 250 and 340 cm^{-1} in Figure 3a and between 200 and 250 cm^{-1} in Figure 3b. After the H_2O_2 treatment, most of the M1 RBM peaks in Figure 3b survived, while all M1 peaks in Figure 3a disappeared. Since the M1 peaks in Figure 3a are minor components in the sample, even after the H_2O_2 treatment, the main component of the RBM spectrum of metallic SWCNT was not changed. On the other hand, in the case of semiconductors, the most intense RBM peak of the S3 band at 229 cm^{-1} in Figure 3a was decreased drastically after the H_2O_2 treatment,

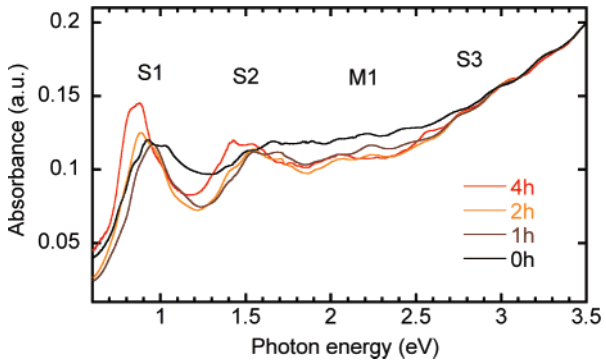

Figure 4. UV−vis−NIR absorption spectra of the SWCNT thin film oxidized in air at different heating times.

and the main component was changed to 196 cm^{-1}. This result means that the diameter distribution of semiconducting SWCNTs has been strongly modified by the H_2O_2 treatment. In a rough diameter estimation from the RBM spectra, the mean diameter of semiconducting SWCNTs changed from 1.0 to 1.2 nm, while the metallic SWCNTs were changed to slightly larger diameters. The corresponding result was observed in G-bands. In Figure 3a, the starting material has weak but apparent broad Raman intensity around 1550 cm^{-1} that is a Breit−Wigner−Fano (BWF) component due to the resonance of the metallic SWCNTs.[17] After the H_2O_2 treatment, since all the metallic resonance disappeared, the BWF component disappeared, and the G-band showed a characteristic spectrum of semiconducting SWCNTs. In contrast, Figure 3b shows a typical BWF spectrum for the H_2O_2-treated SWCNTs, which means that most of the SWCNTs on resonance are metallic. According to the Raman excitation analysis,[22] the semiconducting SWCNTs with 1.0-nm diameters have the S2 absorption bands at 1.6 eV. Indeed, as shown in Figure 2, a corresponding decrease in the optical absorption intensity at 1.6 eV was observed after the H_2O_2 treatment. The peak position of the S2 absorption band of the H_2O_2-treated SWCNTs is 1.4 eV, which corresponds to the S2 absorption of semiconducting SWCNTs with 1.2-nm diameters. In conclusion, it can be said that the Raman results are completely consistent with the result of the optical absorption spectra as discussed in the previous section.

A broad peak around 1350 cm^{-1} is attributed to the Raman mode concerning the defects of the graphitic materials[24] (D-band). A ratio between the G-band and the D-band, *G*/*D*, is a good indicator to discuss the defects and the purity of the SWCNTs. As shown in Figure 3a,b, *G*/*D* values were not changed after the H_2O_2 treatment for both excitation energies. This means that defects in SWCNTs were not enhanced by the treatment. This is understandable because the defective SWCNTs should burn more rapidly than the defectless ones. Even though H_2O_2 induces defects in SWCNTs, a concentration of defects in survived SWCNTs should be conserved at equilibrium.

A similar study was also performed on a thin film of starting SWCNTs as a reference in order to confirm whether the experimental results are representative of a normal oxidation process. Figure 4 shows optical absorption spectra of the SWCNT thin film oxidized in air at different heating times (the spectra were normalized at 3.5 eV). In this case, the S1, S2, and M1 absorption peaks all reflect similar oxidation processes. In accordance with previous observations, it was observed that the thinner SWCNTs were oxidized more rapidly than the larger-diameter SWCNTs. Moreover, there was little difference observed in the removal rates of semiconducting and metallic SWCNTs in the oxidation process in air.

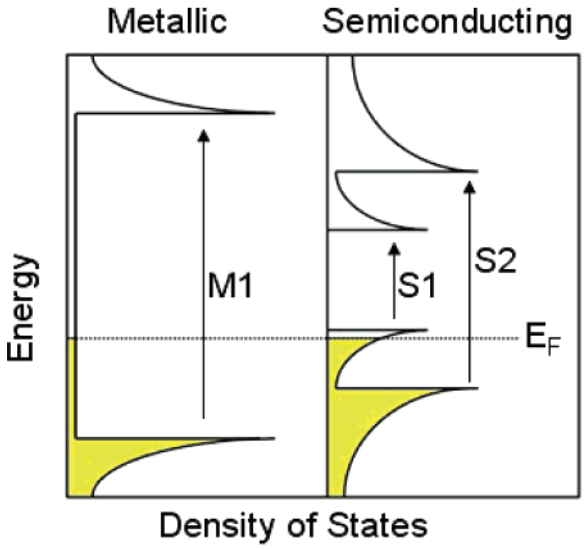

Figure 5. A schematic illustration of the density of states of metallic and semiconducting SWCNTs. Arrows between singularities represent electronic transitions responsible for the S1, S2, and M1 absorption bands. The shadow (yellow) indicates the occupied state.

These results strongly suggest that the semiconducting SWCNTs were selectively oxidized by heat treatment in H_2O_2. However, the small quantity of sample remaining indicates this selectivity is not strict, and the selective oxidation of semiconducting SWCNTs in H_2O_2 is probably caused by their faster oxidation with respect to metallic SWCNTs.

The concentration of metallic SWCNTs in the sample was estimated from the optical absorption spectra. An integrated intensity ratio of the intrinsic absorption bands M1 and S2, M1/(M1 + S2), was estimated by assuming that the superposing absorption due to π-plasmons is linear with respect to the excitation photon energy. It was not possible to determine the intensity ratio of M1 and S2 for raw HiPco because of the broad absorption bands due to a wide diameter distribution. The ratios of the laser ablation and arc discharge samples were determined to be approximately 0.3, which coincidently is comparable with the natural concentration based on the assumption of a random distribution of chirality, where $^1/_3$ of the SWCNTs are metallic. This ratio is tentatively used as a representative indicator of the concentration of metallic and semiconducting SWCNTs within the sample. Here, the absorption intensity ratio for H_2O_2-treated HiPco (for 47 min) was found to be 0.85, indicating that over 80% of the SWCNTs in the sample are metallic.

The following discussion investigates the reasoning behind why semiconducting SWCNTs are selectively removed in H_2O_2. In general, it is expected that metallic SWCNTs have a higher chemical reactivity than semiconducting SWCNTs because of the finite density of state (DOS) at the Fermi level. Indeed, Strano et al. have shown that diazonium salts react selectively with metallic SWCNTs.[25] In our experiment, however, the semiconducting SWCNTs appear to have a higher chemical reactivity. Under the assumption that this chemical reactivity depends on DOS at the Fermi level, it is suggested that the semiconducting SWCNT DOS (at the Fermi level) in H_2O_2 is higher than the corresponding metallic SWCNT DOS. It is well-known that hydrogen peroxide acts as a weak hole-dopant. If the Fermi level shifts to the first vHS band of semiconducting SWCNTs through hole-doping, as shown in Figure 5, then the semiconducting SWCNT DOS (at the Fermi level) should be higher than that observed for metallic SWCNTs. Therefore, it is expected that semiconducting SWCNTs have a higher chemical reactivity in H_2O_2 than metallic SWCNTs.

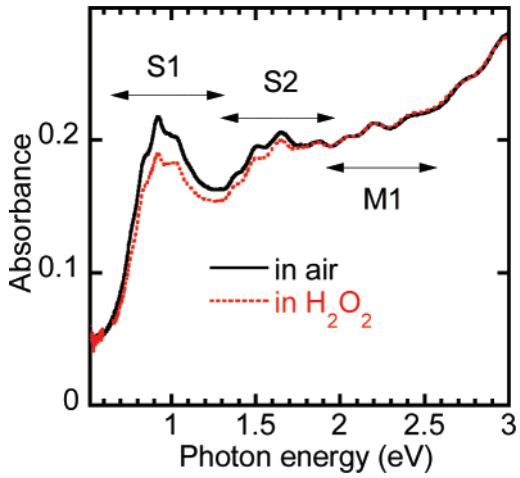

Figure 6. UV−vis−NIR absorption spectra of the SWCNT film in air (dotted line) and H_2O_2 (solid line).

To confirm the electronic state of SWCNTs in H_2O_2, we measured the optical absorption spectra of the purified HiPco film in air and in H_2O_2, as shown in Figure 6. By comparing the two spectra, it is clear that the S1 absorption of the sample in H_2O_2 decreased, while the M1 absorption showed no change. The suppressed optical transition of the S1 band is probably caused by a reduction of DOS for the first vHS band due to hole-doping by H_2O_2.[20] This strongly suggests that the electronic state shown in Figure 5 is more or less realized in the oxidation process in H_2O_2. The holes doped with H_2O_2 cause a lowering of the SWCNT Fermi level, while raising the semiconducting SWCNTs DOS to above those of the metallic SWCNTs. As a result, the higher DOS at Fermi level induced a higher reactivity, affording a greater selective oxidation of semiconducting SWCNTs.

In conclusion, the optical absorption spectra of SWCNTs measured at different heating times in H_2O_2 reveal that hydrogen peroxide oxidizes the semiconducting SWCNTs more favorably than metallic SWCNTs. It can be seen that the H_2O_2-induced oxidation of SWCNTs is good from two perspectives: the low-temperature combustion of SWCNTs without the formation of byproducts and the enhanced chemical reactivity of SWCNTs afforded by hole-doping. Thus, SWCNT oxidation by H_2O_2 is more effective for thinner semiconducting SWCNTs, because of the higher chemical reactivity resulting from curvature effects and the higher DOS (at the Fermi level) caused by hole-doping. In the present work, it was shown that the final concentration of metallic SWCNTs was found to be greater than 80%. Moreover, a higher yield and higher concentration of metallic SWCNTs is expected through homogeneous reactions using isolated SWCNTs.[19] Finally, we would like to point out that this method has a possibility of higher reactivity control through doping. The pH control[26] and the encapsulation of molecules[27] can extend the Fermi level control, realizing a higher selective reactivity between SWCNTs and H_2O_2.

Acknowledgment. We thank Professor J. E. Fisher for helpful discussions. This work was partly supported by the Industrial Technology Research Grant Program in 2003 from New Energy and Industrial Technology Development Organization (NEDO) of Japan. A part of this work was conducted at the AIST Nano-Processing Facility, supported by "Nanotechnology Support Project" of the Ministry of Education, Culture, Sports, Science and Technology (MEXT), Japan.

References and Notes

(1) Hamada, N.; Sawada, S.; Oshiyama, A. *Phys. Rev. Lett.* **1992**, *68*, 1597.

(2) Yao, Z.; Kane, C. L.; Dekker, C. *Phys. Rev. Lett.* **2000**, *84*, 2941.

(3) Tans, S. J.; Verschueren, A. R. M.; Dekker, C. *Nature (London)* **1998**, *393*, 49.

(4) Chen, Y.-C.; Raravikar, N. R.; Schadler, L. S.; Ajayan, P. M.; Zhao, Y.-P.; Lu, T.-M.; Wang, G.-C.; Zhang, X.-C. *Appl. Phys. Lett.* **2002**, *81*, 975.

(5) Sakakibara, Y.; Tatsuura, S.; Kataura, H.; Tokumono, M.; Achiba, Y. *Jpn. J. Appl. Phys.* **2003**, *42*, L494.

(6) Zheng, M.; Jagota, A.; Semke, E. D.; Diner, B. A.; Mclean, R. S.; Lustig, S. R.; Richardson, R. E.; Tassi, N. G. *Nat. Mater.* **2003**, *2*, 338.

(7) Krupke, R.; Hennrich, F.; Löhneysen, H. V.; Kappes, M. M. *Science* **2003**, *301*, 344.

(8) Chen, Z.; Du, X.; Du, M.; Rancken, C. D.; Cheng, H.; Rinzler, A. G.; *Nano Lett.* **2003**, *3*, 1245.

(9) Chattopadhyay, D.; Galeska, I.; Papadimitrakopoulos, F. *J. Am. Chem. Soc.* **2003**, *125*, 3370.

(10) An, K. H.; Park, J. S.; Young, C. M.; Jeong, S. Y.; Lim, S. C.; Kang, C.; Son, J. H.; Jeong, M. S.; Lee, Y. H. *J. Am. Chem. Soc.* **2005**, *127*, 5196.

(11) Maeda, Y.; Kimura, S.; Kanda, M.; Hirashima, Y.; Hasegawa, T.; Wakahara, T.; Lian, Y.; Nakahodo, T.; Tsuchiya, T.; Akasaka, T.; Lu, J.; Zhang, X.; Gao, Z.; Yu, Y.; Nagase, S.; Kazaoui, S.; Minami, N.; Shimizu, T.; Tokumoto, H.; Saito, R. *J. Am. Chem. Soc.* **2005**, *127*, 10287.

(12) Rosen, R.; Simendinger, W.; Debbault, C.; Shimoda, H.; Fleming, L.; Stoner, B.; Zhou, O. *Appl. Phys. Lett.* **2000**, *76*, 1668.

(13) Liu, J.; Rinzler, A. G.; Dai, H.; Hafner, J. H.; Bradley, R. K.; Boul, P. J.; Lu, A.; Iverson, T.; Shelimov, K.; Huffman, C. B.; Rodriguez-Macias, F.; Shon, Y. S.; Lee, T. R.; Colbert, D. T.; Smalley, R. E. *Science* **1998**, *280*, 1253.

(14) Yudasaka, M.; Zhang, M.; Iijima, S. *Chem. Phys. Lett.* **2003**, *374*, 132.

(15) Simon, F.; Kukovecz, A.; Kuzmany, H. *AIP Conf. Proc.* **2003**, *685*, 185.

(16) Wu, Z.; Chen, Z.; Du, X.; Logan, J. M.; Sippel, J.; Nikolou, M.; Kamaras, K.; Reynolds, J. R.; Tanner, D. B.; Hebard, A. F.; Rinzler, A. G. *Science* **2004**, *305*, 1273.

(17) Kataura, H.; Kumazawa, Y.; Maniwa, Y.; Umezu, I.; Suzuki, S.; Ohtsuka, Y.; Achiba, Y. *Synth. Met.* **1999**, *103*, 2555.

(18) Nagasawa, S.; Yudasaka, M.; Hirahara, K.; Ichihashi, T.; Iijima, S. *Chem. Phys. Lett.* **2000**, *328*, 374.

(19) O'Connell, M. J.; Bachilo, S. M.; Huffman, C. B.; Moore, V. C.; Strano, M. S.; Haroz, E. H.; Rialon, K. L.; Boul, P. J.; Noon, W. H.; Kittrell, C.; Ma, J.; Hauge, R. H.; Weisman, R. B.; Smalley, R. E. *Science* **2002**, *297*, 593.

(20) Kazaoui, S.; Minami, N.; Jacquemin, R.; Kataura, H.; Achiba, Y. *Phys. Rev. B* **1999**, *60*, 13339.

(21) Saito, R.; Dresselhaus, G.; Dresselhaus, M. S. *Physical Properties of Carbon Nanotubes*; Imperial College Press: London, 1998.

(22) Fantini, C.; Jorio, A.; Souza, M.; Strano, M. S.; Dresselhaus, M. S.; Pimenta, M. A. *Phys. Rev. Lett.* **2004**, *93*, 147406.

(23) Jorio, A.; Santos, A. P.; Ribeiro, H. B.; Fantini, C.; Souza, M.; Vieira, J. P. M.; Furtado, C. A.; Jiang, J.; Saito, R.; Balzano, L.; Resasco, D. E.; Pimenta, M. A. *Phys. Rev. B* **2005**, *72*, 075207.

(24) Reich, S.; Thomsen, C.; Maultzsch. J. *Carbon Nanotubes: Basic Concepts and Physical Properties*; Wiley: New York, 2004.

(25) Strano, M. S.; Dyke, C. A.; Usrey, M. L.; Barone, R. W.; Allen, M. J.; Shan, H.; Kittrell, C.; Hauge, R. H.; Tour, J. M.; Smalley, R. E. *Science* **2003**, *301*, 1519.

(26) Zhao, W.; Song, C.; Pehrsson, R. E. *J. Am. Chem. Soc.* **2002**, *124*, 12418.

(27) Takenobu, T.; Takano, T.; Shiraishi, M.; Murakami, Y.; Ata, M.; Kataura, H.; Achiba, Y.; Iwasa, Y. *Nat. Mater.* **2003**, *2*, 683.